Published 1982 by El:
NUMERICAL GRID GENERATION
Joe F. Thompson, editor

A VECTORIZED, FINITE-VOLUME, ADAPTIVE-GRID ALGORITHM FOR NAVIER-STOKES CALCULATIONS

PETER A. GNOFFO[+]

[+]Aero-Space Technologiet, Aerothermodynamics Branch, Space Systems Division, NASA Langiey Research Center, Hampton, Virginia 23665, Graduate Student, Department of Mechanical and Aeroepace Engineering, Pr.nceton Univereity.

ABSTRACT

An adaptive grid, finite-volume method hae been used to solve the Navier-Stokee equations for complete (forebody and afterbody) flowfielde around blunt bc lies. The code, which is applicable for axisymmetric cr two-dimensional flows, allows the meeh to adjust during the computation to provide a closer spacing of mesh points in regione of high gradiente, thus minimizing the number of required computational points. The solution technique is explicit, utilizing a maximum time-step advancement at each grid point to accelerate convergence to the eteady state. The code has been fully vectorized for efficient eolution on the CYBER 203 computer. A very flexible rezoning routine ie ueed to concentrate mesh pointe anywhere in the field, either by a ueer-defined weighting function or by allowing high gradient regions to adjust the grid. The grid adjuetment routine is implicit in nature and represents a very emall portion cf the total computat:onal coet. Currently, the code rune in approximately 1.6 × 10^{-5} = 0.00001 seconds per grid point per iteration.

INTRODUCTION

The finite-volume method of numerically eolving syetems of coneervation laws has been successfully applied to a wide variety of problems in fluid mechanics.[1-6] Its ability to maintain conservetion of mass, momentum, and energy from cell to cell, even in rether complex nonorthogonal coordinatee, makee it particularly attractive for use with adaptive grid techniquee. For the purpoeee cf this paper, a finite-volume formulation (FVF) ie defined as a diecrete approximation to a conservation law written in integral form which (1) uniquely defines control volumes in such a way that control volumee (ceiie) do not overlap nor are gape left in phyeical spece and (2) uniquely definee fluxee and forces acting through cell walls so that summability without residue[7] (coneervation) ie guaranteed. It differs from a finite difference formulation (FDF) only in the way a problem is approached. For example, given a syetem of coneervetion lawe we might consider the FDF as a discrete approximation to the differential form of the laws while the FVF is a discrete approximation to the integral form of the laws. A review of various FVF's suggests that all FVF's can be written as FDF's (and usually appear that way in the literature) but not all FDF's can be written as FVF's. Furthermore, discretizing the divergence form[8] of the conservation laws in general coordinates to obtain the FDF does not guarantee that the formulation can be expressed as an FVF because conservation is not maintained due to some confusion of how to properly define the metric coefficients. Various ways of defining the metric coefficients to overcome this problem have been given in References 5 and 9. The discussion there leads one to conclude that while there may be a certain amount of ambiguity in how to properly define or discretize the metrics the problems can be overcome without a great deal of difficulty. It should also be noted that the FDF of a conservation law written in nondivergence form can in fact be a conservative FVF. An example of such a scheme is presented in Reference 10.

The discussion up to this point has been concerned with taking a differential form of a conservation law, approximating it by an FDF, and testing if it satisfies the requirements of an FVF (or forcing it to satisfy the requirements by suitably defining the metrics). The approach taken in the presentation which follows is to start with the integral form of the conservation law, approximate it with an FVF on some generalized grid, and expand the formulation to see what FDF results. It will be shown that no special treatment of metrics is required and in fact no terms which are readily recognizable as metric coefficients ever appear. It is only when the FVF is expanded into a format more familiar as an FDF do these metrics appear as ratios of the dimensions of cell walls to cell volumes. Furthermore, the unexpanded form of the FVF is ideally suited for vectorization.

Within this framework a grid adaption routine has been developed which greatly facilitates placement of mesh points where needed. A description of how the adaption algorithm has evolved from the groundwork established in references 11 and 12 to the current implicit adaption scheme will be presented. Finally, sample calculations of supersonic flow over a Viking Aeroshell, including flow in the wake, demonstrate the versatility of both the FVF and the adaption algorithm through its ability to concentrate points not only in the boundary layer but also in the free shear layer.

FINITE-VOLUME FORMULATION

Consider a system of two-dimensional conservation laws which can be expressed by the vector relation

$$\frac{\partial U}{\partial t} + \frac{\partial F}{\partial x} + \frac{\partial G}{\partial y} = 0 \tag{1a}$$

$$\iiint \frac{\partial U}{\partial t}\, dv + \iint (F\bar{i} + G\bar{j}) \cdot \bar{ds} = 0 \tag{1b}$$

where Equations (1a) and (1b) are the differential and integral forms of the conservation laws respectively, and $\bar{i}$ and $\bar{j}$ are unit vectore in the x and y directions, respectively.

A control volume in two-dimeneional (or axieymmetric) space is determined by a quadrilateral whoee vertices are defined by adjacent mesh points. The [i,j] cell refere to the cell with verticee (i,j), (i+1,j), (i,j+1), (i+1,j+1). Pointe of constant j index define ξ coordinate linee, increasing ξ in the direction of increasing i. Points of constant i index define η coordinate lines, increaeing η in the direction of increasing j (eee Fig. 1). The flux through the wall defined by the points <(i,j), (i,j+1)> ie calculated using information from the (i,j) vertex on the predictor step and from the (i,j+1) vertex on the corrector etep for odd time steps. The order is revereed for even time stepe. The flux through the wall defined by the points <(i,j), (i+1,j)> follows a similar pattern of definition, ueing information from the (i,j) vertex on the predictor step. The FVF for the [i,j] cell is written:

$$\begin{aligned}\left.\frac{\partial U}{\partial t}\right|_{i,j}^{\overline{n+1}} A_{i,j} &+ F^n_{i+1,j}(y_{i+1,j+1} - y_{i+1,j}) - G^n_{i+1,j}(x_{i+1,j+1} - x_{i+1,j}) \\ &- F^n_{i,j}(y_{i,j+1} - y_{i,j}) + G^n_{i,j}(x_{i,j+1} - x_{i,j}) \\ &- F^n_{i,j+1}(y_{i+1,j+1} - y_{i,j+1}) + G^n_{i,j+1}(x_{i+1,j+1} - x_{i,j+1}) \\ &+ F^n_{i,j}(y_{i+1,j} - y_{i,j}) - G^n_{i,j}(x_{i+1,j} - x_{i,j}) = 0\end{aligned} \tag{2a}$$

$$\left.\frac{\partial U}{\partial t}\right|_{i,j}^{\overline{n+1}} A_{i,j} + \overline{F^{n+1}}_{i+1,j+1}(y_{i+1,j+1} - y_{i+1,j}) - \overline{G^{n+1}}_{i+1,j+1}(x_{i+1,j+1} - x_{i+1,j})$$
$$- \overline{F^{n+1}}_{i,j+1}(y_{i,j+1} - y_{i,j}) + \overline{G^{n+1}}_{i,j+1}(x_{i,j+1} - x_{i,j})$$
$$- \overline{F^{n+1}}_{i+1,j+1}(y_{i+1,j+1} - y_{i,j+1}) + \overline{G^{n+1}}_{i+1,j+1}(x_{i+1,j+1} - x_{i,j+1})$$
$$+ \overline{F^{n+1}}_{i+1,j}(y_{i+1,j} - y_{i,j}) - \overline{G^{n+1}}_{i+1,j}(x_{i+1,j} - x_{i,j}) = 0 \qquad \text{(2b)}$$

$$U_{i,j}^{n+1} = .5\left(\overline{U_{i,j}^{n+1}} + \overline{\overline{U_{i,j}^{n+1}}}\right) \qquad \text{(3)}$$

where A_{ij} is the eree of the $[i,j]$ cell. Equetion (2) must epproximate the integrel form of Equetion (1). The firet term of Equetion (2) must epproximate the integrel of $\partial U/\partial t$ over the entire cell. In the FVF we eet

$$\left.\frac{\partial U}{\partial t}\right|_{i,j}^{\overline{n+1}} = \frac{\overline{U_{i,j}^{n+1}} - U_{i,j}^{n}}{\Delta t_{ij}} \qquad \text{(4e)}$$

$$\left.\frac{\partial U}{\partial t}\right|_{i,j}^{\overline{n+1}} = \frac{\overline{U_{i+1,j+1}^{n+1}} - U_{i+1,j+1}^{n}}{\Delta t_{i+1,j+1}} \qquad \text{(4b)}$$

Note the uee of a Δt which veries from point to point in Equation (4).

Now coneider e finite-difference formulation, FDF, of Equation (1) which can be trensformed to

$$\frac{\partial U}{\partial t} + \frac{\partial F}{\partial \xi}\frac{\partial \xi}{\partial x} + \frac{\partial F}{\partial \eta}\frac{\partial \eta}{\partial x} + \frac{\partial G}{\partial \xi}\frac{\partial \xi}{\partial y} + \frac{\partial G}{\partial \eta}\frac{\partial \eta}{\partial y} = 0 \qquad \text{(5)}$$

where $x = x(\xi,\eta)$, $y = y(\xi,\eta)$. The FDF of (5) is written:

$$U^{\overline{n+1}}_{i,j} = U^n_{i,j} - \Delta t_{i,j}\left[\frac{(F_{i+1,j} - F_{i,j})^n}{\Delta\xi}\,\xi^+_{x_{ij}} + \frac{(G_{i+1,j} - G_{i,j})^n}{\Delta\xi}\,\xi^+_{y_{ij}} + \frac{(F_{i,j+1} - F_{i,j})^n}{\Delta\eta}\,\eta^+_{x_{ij}} + \frac{(G_{i,j+1} - G_{i,j})^n}{\Delta\eta}\,\eta^+_{y_{ij}}\right] \tag{6a}$$

$$U^{\overline{\overline{n+1}}}_{i,j} = U^n_{i,j} - \Delta t_{i,j}\left[\frac{(F_{i,j} - F_{i-1,j})^{\overline{n+1}}}{\Delta\xi}\,\xi^-_{x_{ij}} + \frac{(G_{i,j} - G_{i-1,j})^{\overline{n+1}}}{\Delta\xi}\,\xi^-_{y_{ij}} + \frac{(F_{i,j} - F_{i,j-1})^{\overline{n+1}}}{\Delta\eta}\,\eta^-_{x_{ij}} + \frac{(G_{i,j} - G_{i,j-1})^{\overline{n+1}}}{\Delta\eta}\,\eta^-_{y_{ij}}\right] \tag{6b}$$

$$U^{n+1}_{i,j} = \frac{1}{2}\left(U^{\overline{n+1}}_{i,j} + U^{\overline{\overline{n+1}}}_{i,j}\right) \tag{6c}$$

The FVF (Eqs. (2) and (4)) and the FDF (Eq. (6)) are equivalent if

$$\xi^+_{x_{ij}} \equiv (y_{i+1,j+1} - y_{i+1,j})\ \Delta\xi/A_{ij} \tag{7a}$$

$$\eta^+_{x_{ij}} \equiv (y_{i,j+1} - y_{i+1,j+1})\ \Delta\eta/A_{ij} \tag{7b}$$

$$\xi^+_{y_{ij}} \equiv (x_{i+1,j} - x_{i+1,j+1})\ \Delta\xi/A_{ij} \tag{7c}$$

$$\eta^+_{y_{ij}} \equiv (x_{i+1,j+1} - x_{i,j+1})\ \Delta\eta/A_{ij} \tag{7d}$$

$$\xi^-_{x_{ij}} \equiv (y_{i-1,j} - y_{i-1,j-1})\ \Delta\xi/A_{i-1,j-1} \tag{7e}$$

$$\eta^-_{x_{ij}} \equiv (y_{i-1,j-1} - y_{i,j-1})\ \Delta\eta/A_{i-1,j-1} \tag{7f}$$

$$\xi^{-}_{y_{ij}} \equiv (x_{i-1,j-1} - x_{i-1,j})\ \Delta\xi/A_{i-1,j-1} \qquad (7g)$$

$$\eta^{-}_{y_{ij}} \equiv (x_{i,j-1} - x_{i-1,j-1})\ \Delta\eta/A_{i-1,j-1} \qquad (7h)$$

A linearized analysis of the FDF (Eq. (6)), after it has been expanded into a one-step scheme shows the following: (1) Equation (6) is a consistent representation of Equation (5), (2) the truncation error for variable Δt_{ij} is first order in time and can be expressed

$$E_1 = \frac{-\Delta t_{ij}}{2}\left(\frac{\partial h_{ij}}{\partial\xi} C + \frac{\partial h_{ij}}{\partial\eta} D\right)\left(C\frac{\partial U}{\partial\xi} + D\frac{\partial U}{\partial\eta}\right) \qquad (8)$$

where

$$C = \frac{\partial F}{\partial U}\xi_x + \frac{\partial G}{\partial U}\xi_y,\ D = \frac{\partial F}{\partial U}\eta_x + \frac{\partial G}{\partial U}\eta_y$$

and

$$h_{ij}(\xi,\eta) = \Delta t(\xi,\eta)/\Delta t(\xi_{ij},\eta_{ij})$$

Note that $E_1 = 0$ if Δt_{ij} = constant, and (3) the spatial truncation error is of $O(\Delta^2)$ where Δ is proportional to a cell wall dimension if all $\xi^{\pm}_x$, etc., are first-order-accurate approximations to ξ_x, etc., and $(\xi^{+}_x + \xi^{-}_x)/2$, etc., are second-order-accurate approximations to ξ_x, etc. These conditions are formally satisfied by Equation (7). For example

$$(\xi^{+}_x + \xi^{-}_x)/2 = \xi_x + \Delta\xi\{\Delta\xi\ [(Jy_{\xi\eta})_\xi + Jy_{\xi\xi\eta}] + \Delta\eta(Jy_{\xi\eta})_\eta\}/2 \qquad (9)$$

where $J = x_\xi y_\eta - x_\eta y_\xi$.

Consequently, it is seen that while the FDF or FVF is second-order-accurate (for Δt_{ij} = constant) excessive stretching or skewness of the grid can introduce large factors of second-order terms. Furthermore, these factors multiply terms like $\partial^2 U/\partial\xi^2$, etc., and they contribute to the overall artificial viscosity of the method. At present, grid-induced errors are checked by comparing rssults obtainsd for ths ssme problsm on ths differsnt grids constructsd from mors points or from diffsrsnt adjusting paramstsrs (sss section on ADAPTIVE GRID). It should slso be noted thst whils Equstion (5) is not in strict conssrvation form, ths FVF which modsls Equstion (1b) is conssrvstive in ths strict senss of summation without rssidus.[7] For exampls, regardless of the grid used, the FVF returns an exact uniform flow if s uniform flow is used as an initisl condition.

It is notsd thst the equations and anslysis in this section srs for two-dimensionsl flow. An axisymmetric sxtsnsion introducss only minor complicstions. Finally we point out thst ths FVF (Eqs. (2) snd (4)) reduces to MacCormack's method[13] in Cartssian coordinstes. There sre sn infinity of other wsys to define cells and flux through cells on s genersl grid, ssch of which lead to s unique FVF and uniqus dsfinitions of metric coefficients for thst particulsr FVF.

BOUNDARY CONDITIONS

Only s cursory description of boundsry conditions can be provided due to space limitstions.

Well: $u = v = 0$.
Adiabatic wsll or constant wall tempersturs. $\partial p/\partial n = 0$.
(n coordinsts normal to wsll)

Shock: Rankine-Hugoniot relstions for s discrsts moving shock sre epplied. Pressurs behind shock obtained from extrspoletion from intsrior points.

Symmetry: Limiting form of differsntisl form of govsrning equstions solved using MacCormack's method.

Outflow: Primitive variables obteined by sxtrepolstion.

ADAPTIVE GRID

Ths prssent grid edjustment schsme has evolved from ons which imparted velocitiss to grid points based on gradients in the fisld ss in Referencss 11 and 12 to one which rezones the computationel mesh using an implicit algorithm at any desired frequency (i.e., once per time stsp or once per 1000 time stsps). Originelly svery point (i,j) in ths computational plans wes connected to the four adjecent points (i±1,j), (i,j±1) by springs whoss spring constants K_i^j, K_j^i were determined by s function of the gredient of some dependent variable between the points. For exampls, the spring slong the ith row connscting points (i,j) and (i,j+1) was defined

$$K_j^i = 1 + c|f_{i,j} - f_{i,j+1}|/\Delta\bar{r} \tag{10}$$

where c is a conetant and $\Delta\bar{r}$ is the distance between the points. Grid points on the boundariee were free to move along the boundary as if on a frictionlese rod. Grid points on the corners of the domain were held fixed. Small adjuetmente in the x and y directione were aseigned to grid points as determined by the net forcee on the grid points in the reepective directions. After every time step, the grid was updated and checked to make sure that no grid overlap was imminent.

In a noninteractive teet case where $p(x,y)$ was prescribed to model the preseure field of an oblique shock crossing a uniform flowfield $(p(t) \equiv 0)$, the grid evolved from one of equally epaced rectangular celle to the one shown in Figure 2. In an inteiactive teet caee where the solution $p(x,y,t)$ was allowed to evolve with time, the final grid distribution (Fig. 3) is eeen to be much more erratic than that of the previoue caee. The preseure field for this case is shown in Figure 4.

By sacrificing the column to column (or row to row) influence of the epring system (i.e., no springs between column i and column i+1) a euperior algorithm in terms of computational coste and smoothnees of grid dietribution can be constructed. (Smoothneee of grid distribution is a eubjective judgment. A coordinate line whose direction or length changee erratically from point to point is judged nonsmooth.)

Consider the coordinate line of constant index i as shown in Figure 5.

(11)

Let $f_{j,m}$ be a table of dependent variablee at the point e_j defined by

$$f_{j,1} = x_j,\ f_{j,2} = y_j,\ f_{j,3} = \rho_j,\ f_{j,4} = u_j,\ f_{j,5} = v_j,\ f_{j,6} = e_j \tag{12}$$

The grid pointe in physical (x,y) space are mapped onto a etraight line in s space. Let each grid point be connected to its neighbor in s space by a epring with spring constant K_j between the j and j+1 points to be defined later.

Let Δn_j be the listance between tha j and j+1 points in s epace. Then $K_j \Delta n_j$ equals a constant. Therefore,

$$\Delta n_j = K_1 \Delta n_1/K_j \tag{13}$$

The known total length of s can be expressed as

$$s_{JN+1} = \sum_{j=1}^{JN} \Delta n_j = \Delta n_1 K_1 \sum_{j=1}^{JN} 1/K_j = \Delta n_1 K_1 \text{ SUM} \tag{14}$$

whare JN = total number of intervals. Coneequently,

$$\begin{aligned} \Delta n_1 &= s_{JN+1}/(K_1 \text{ SUM}) \\ \Delta n_j &= s_{JN+1}/(K_j \text{ SUM}) \end{aligned} \tag{15}$$

The constants K_j can be definad explicitly or implicitly. An axplicit definition of K_j assigns a value to the spring conetant independent of the poeition of the epring in e epaca. For exampla,

$$K_j = \exp(-c_1 \cdot j/JN) \tag{16}$$

provides an exponantially increasing spacing of grid points from j = 1 to j = JN where the conetant c_1 is used to control stretching. Thie definition provides no adaptive capability but doee provide a very quick way of concentrating points near boundarias.

An implicit dafinition of K_j assigns a value to the spring constant which ie a function of the position of the spring in s space. For an implicit case, the algorithm is implemented ae followe:

(1) Start at the firet column (or row) of data and compute and etora all the values of s_j and $f_{j,m}$.

(2) Initialize $\bar{n}_j$ and n_j equal to s_j for all j, ITER = 0.

(3) Sat ITER = ITER + 1.

(4) Ueing the known stored values of indapendent variable s_j and dapendent variables $f_{j,m}$, compute the new values of the dapendent variables $d_{j,m}$ at all n_j with a univariata intarpolation routine whare $d_{j,1} = x_j$, $d_{j,2} = y_j$, etc.

(5) Compute $K_j = K_j(d_{j,m})$.

6) Compute the new coordinatee n_j from Equation (15); set $n_{JN+1} = e_{JN+1}$ to keep end point valuee unchanged.

(7) Compute an error norm to determine convergence

$$L_2 = \sum_{j=2}^{JN} (n_j - \bar{n}_j)^2 \, ^{1/2} \tag{17}$$

If $L_2 < 0.0001$, proceed to etep (9).

If ITER > 100, stop the procedure.

(8) Set $\bar{n}_j = n_j$ for all j and go to step (3).

(9) Replace x_j, y_j, ρ_j, etc., with $d_{j,1}$, $d_{j,2}$, $d_{j,3}$, etc., go to next column of data and repeat all etepe.

Typical definitione of K_j employ gradients of velocity, internal energy, or Mach number. For example,

$$K_j = 1 + c_3 |e(n_{j+1}) - e(n_j)| / (n_{j+1} - n_j) \tag{18}$$

where c_3 can be ueed to control the concentration of mesh points in regions of high gradient. Examples of grid dietribution using these gradient adaptive mechanisms will be presented in the RESULTS section.

In caees where a high gradient develops rapidly, ae in the vicinity of an expaneion corner of a planetary probe, the adaption algorithm can have trouble converging. Thie problem is overcome as follows.

(1) After step (4) in the adaption algorithm, the overall change in the new grid distribution n_j is damped by writing

$$n_j = c_4 n_j + (1 - c_4)\bar{n}_j \tag{19}$$

where $0 < c_4 \leq 1$ (c_4 ie typically of order 1/2)

(2) After etep (5) in the adaption algorithm, the values of the spring constants are filtered by writing

$$K_j^{n+1} = (K_{j-1} + 2K_j + K_{j+1})^n/4; \quad j = 2, JN-1 \tag{20}$$

Often the convergence problems can be overcome by keeping the rezoning interval small or by avoiding large changee of c_3 in Equation (18) between rezonings.

The major advantage of the rezoning procedure deecribed herein is that it provides a very quick way of providing an adaptive capability to the finite-volume formulation. The option to control razoning frequency allows the grid to dynamically adapt to developing features of the flow (i.e., shock, ehear layers) and then to be held fixed as steady state is approached. The rezoning procedure can aleo be used as a separate program to etudy the effecte of monitoring various gradiente in the field or using different definitions of κ_j.

RESULTS AND DISCUSSION

Tha finite-volume, adaptive grid algorithm described in the previous sectione hae been ueed to compute supersonic flowfields over spheres, cylindars and two planetary probe configurations. The most ccmpraheneive teste to date for teeting the adaption algorithm have been on the Viking Aeroshell (Fig. 6), a configuration which protacted the Viking lander for its descent through the Martian atmoephere. Thie eection will deal exclusively with those reeulte. The freestream conditione, $M_\infty = 2$, $\gamma = 1.285$, $Re_\infty = 5000$, have besn chosen to permit comparison with the rasults of Referance 14. Subeequent calculatione at higher Reynolds numbere hava been generated to demonetrete the capabilities of the adaption elgorithm.

The grid ahown in Figure 6 was achieved with an explicit definition of κ_j (Eq. (16)) with $c_1/JN = 0.15$, 90 points around the body and down the waka centerline and 31 points betwesn the body/wake centerline and the bow shock. The preseure dietribution around the body/wake centerlina ie preesnted in Figure 7. Thie ceee was run to convergence in approximately 35 minutes of computing time with a timing of $\approx 3 \times 10^{-5}$ sec/itsretion/grid point. Recent changee in the code effecting the manner in which date ere stored have de- creesed timing to $\approx 1.6 \cdot 10^{-5}$ sec/iteration/grid point.

An edaptive grid celculetion which monitored velocity gradients was applied to this eame problem. In the previous caee, the grid wae not eufficiently stretched to adequately reeolve the boundary layer at the aeparation point. Since the separetion region ie very important in determining the nature of the flow in the wake,[15] it was decided to run this ceee with 91 pointe acroea the ehock layer. The converged grid for $c_3 = 0.5$ ie shown in Figure 8. In defining the values of κ_j near the wall, a teet wae included that would make $\kappa_j = 3$, $j \leq 4$ if κ_j waa previouely lees than 3. From $j = 5$ to 9, the minimum ellowable value of κ_j wee decreased linearly to zero. This forcee a concentration of pointe near the body and in the wake. Preeeura dietribution ie plotted in Figure 7. Comparieons with numericel reaulte of

Reference 14 for shock shape and pressure distribution down the wake centerline show generally good agreement in Figures 9 and 7, respectively.

Solutions for the higher Reynolds number cases ($5 * 10^4$, $5 * 10^6$) were generated sequentially using the previous results as initial conditions. All of these results are for laminar flow and so while the highest ones are physically in error they test the adaption routine's ability to resolve the large gradients associated with such flows.

Some interesting results of these high Reynolds number studies are presented in Figures 10 through 17. The converged grid showing a concentration of points in the free shear layer is presented in Figure 10. The streamline pattern around the expansion corner of the vehicle and associated Mach number contours are presented in Figures 11 and 12. The outer extent of these figures is defined by the physical location of the 25th mesh point. The velocity and grid point distributions along the η coordinate line ($i=22$) located just ahead of the expansion corner are given in Figure 13 for $Re_\infty = 10^4$ and 10^6. These results were obtained using twenty passes through Equation (20) with $c_3 = 0.5$ and 1.0 respectively. The global internal energy contour plot in Figure 14 shows the high gradient regions in the shear layer behind the expansion corner, the captured recompression shock in the wake and a small, high gradient shock-like region on the symmetry line just behind the base where recirculating velocities rapidly change from supersonic to subsonic. This phenomenon was also observed in the results of Reference 14 using a different numerical approach. The high gradient free shear layer extends approximately one-fourth maximum body radius beyond the corner after which point the gradients rapidly decrease and the flow turns toward the axis. There is a large region just below the shear layer of low density ($.2 \leq \rho/\rho_\infty \leq .7$) recirculating flow. A Mach number distribution along an η coordinate line ($i=34$), Figure 15, shows the high gradient region and distribution of mesh points through the shear layer. The complexity of the flow in this region and the ability of the adaption process to concentrate mesh points in the high gradient regions away from the wall further demonstrate the versatility and sensitivity of the adaption process.

CONCLUDING REMARKS

The Finite-Volume Formulation (FVF) described herein has been shown to be a consistent and conservative approximation to the Navier-Stokes equations. The formulation has a first order error in wave speed, proportional to the local value of Δt, when the local maximum time step is used to advance the solution at every point. The formulation is second order accurate when constant time increment is used to advance the solution. However, at large Reynolds numbers (small cell volumes) the constant Δt advancement of the solution, using one value of Δt that is stable for all points, is impractical because many more iterations are required to converge the solution. Converged solutions for complete blunt body flows using approximately 3000 mesh points can be obtained within 30 minutes using the variable Δt option and adaptive grid rezoning on the CYBER 203 computer.

In all of the problems considered herein adaption along only one coordinate line is quite sufficient for the purpose of moving mesh points to high gradient regions in the flow. Restricting grid motion along one coordinate direction permits application of a highly efficient implicit grid adaption procedure. The routine can be implemented at any desired frequency thus permitting dynamic adaption or cost savings by adapting only after large increments of iteration count. Grid point concentration in the boundary layer and free shear layer have demonstrated the success and versatility of the adaption algorithm.

REFERENCES

1. Rizzi, Arthur W., Inouye, Mamoru (1973) A Time Split Finite-Volume Technique for Three-Dimensional Blunt Body Flow, AIAA Paper No. 73-133.
2. MacCormack, R. W. and Paullay, A. J. (1974) The Influence of the Computational Mesh on Accuracy for Initial Value Problems with Discontinuous or Nonunique Solutions, Computers and Fluids, Vol. 2, pp. 339-361.
3. Thomas, P. D. and Lombard, C. K. (1978) The Geometric Conservation Law - A Link Between Finite-Difference and Finite-Volume Methods of Flow Computation on Moving Grids, AIAA Paper No. 78-1208.
4. Caughey, D. A. and Jameson A. (1980) Progress in Finite Volume - Calculations for Wing-Fuselage Combinations, AIAA Journal, Vol. 18, No. 11.
5. Lombard, C. K., Davy, W. C. and Green, M. J. (1980) Forebody and Base Region Real Gas Flow in Severe Planetary Entry by a Factored Implicit Numerical Method - Part I (Computational Fluid Dynamics), AIAA Paper No. 80-0065.
6. Allen, J. S. and Cheng, S. I. (1970) Numerical Solutions of the Compressible Navier-Stokes Equations for the Laminar Near Wake, Physics of Fluids, Vol. 13, No. 1, pp. 37-52.
7. Cheng, Sin I. (1974) A Critical Review of the Numerical Solution of Navier-Stokes Equations, Lecture Notes in Physics, No. 41, Springer Verlag, 1974
8. Roache, Patrick J. (1972) Computational Fluid Dynamics, Hermosa Publishers, Albuquerque, New Mexico.
9. Pulliam, T. H. and Steger, J. L. (1978) An Implicit Finite-Difference Simulations of Three-Dimensional Flow, AIAA Paper 78-10.
10. Shubin, Gregory and Cheng, Sin I. (1979) Gas Dynamic Modeling and Computational Accuracy, Journal of Computational Physics, Vol. 32.
11. Dwyer, H. A., Kee, R. J. and Sanders, B. R. (1979) An Adaptive Grid Method for Problems in Fluid Mechanics and Heat Transfer, AIAA Paper No. 79-1464.

12. Rai, M. M. end Anderson, D. A. (1981) The Use of Adaptive Grids in Conjunction with Shock Cepturing Methods, AIAA Paper 81-1012.

13. MacCormack, R. W. (1969) The Effect of Viscosity in Hypervelocity Impect Cratering, AIAA Paper 69-354.

14. Gnoffo, Peter A. (1980) Complete Supersonic Flowfields Over Blunt Bodies in e Generelized Orthogonal Coordinate System, NASA TM 81784.

15. Berger, Stanley A. (1971) Laminar Wakes, American Elsevier Publishing Company, Inc., New York.

Fig. 1 Schematic ehowing reletion of indexing system, physicel (x,y) coordinetes, and computstionel (ξ,η) coordinatee.

Fig. 4 Perepective view of pressure on (x,y) plane for oblique shock celculetion on interective grid.

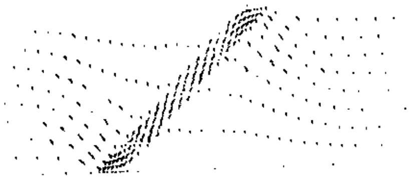

Fig. 2 Nonintsrective example of grid edapting to prescribed prssurs dietribution with two degreee of adaptive freedom.

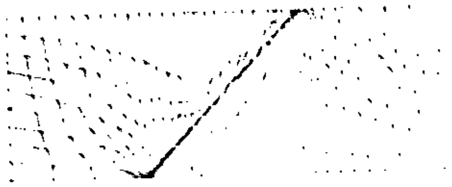

Fig. 3 Intersctive sxampls of grid sdapting tc computsd prsssure distribution scross oblique shock with two degress of sdaptive freedom.

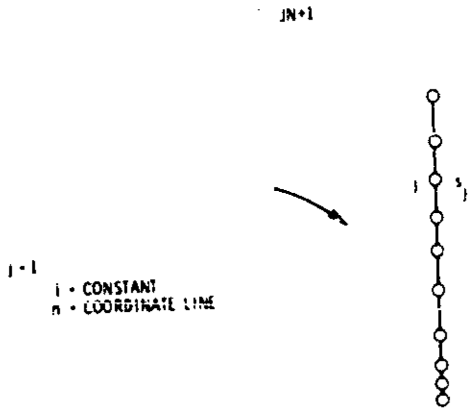

Fig. 5 Schematic ehowing spring system for one degree of sdaptive freedom along η coordinate line.

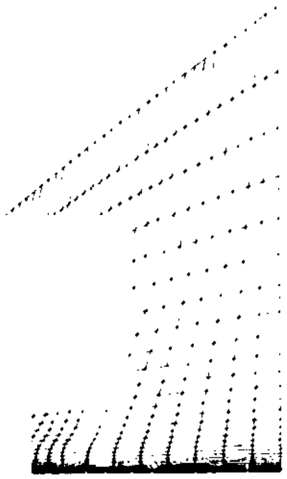

Fig. 6 Grid over Viking Aeroshell obtained with explicit definition of K_j, C_1/JN=.15.

Fig. 8 Grid over Viking Aeroshell obtained with implicit definition of K_j, Re_∞=5000.

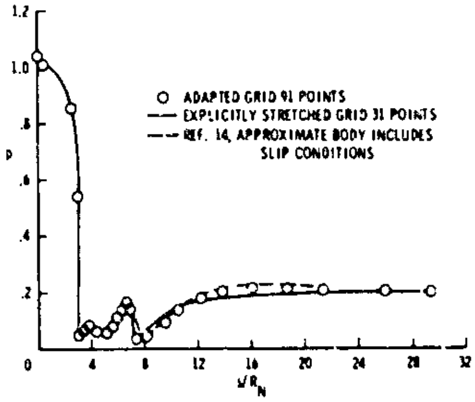

Fig. 7 Pressure distribution eround body/weke centerline of Viking Aeroshell. M_∞=2, Re_∞=5000, γ=1.285.

○ FINITE VOLUME
—— REF. 14

Fig. 9 Bow shock over Viking Aeroshell for M_∞=2, Re_∞=5000.

Fig. 10 Grid over Viking Aeroehell obtained with implicit definition of K_j, Re_∞=10^6.

Fig. 11 Streamlines around expaneion corner of Viking Aeroehell, M_∞=2, Re_∞=10^6.

Fig. 12 Mach number contoure around expaneion corner of Viking Aeroshell, M_∞=2, Re_∞=10^6.

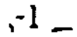

Fig. 13 Velocity and grid specing dietribution along η coordinete line ahead of expansion corner, Re_∞=10^4 and 10^6.

Fig. 14 Contour plot of internel energy over Viking A roshell for $M_\infty=2$, $Re_\infty=10^6$.

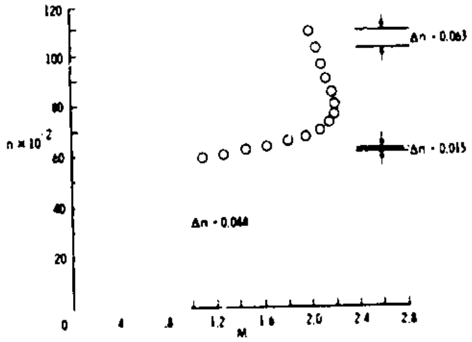

Fig. 15 Mach number and grid specing distribution through sepereted shear layer behind expansion corner along η coordinate line.